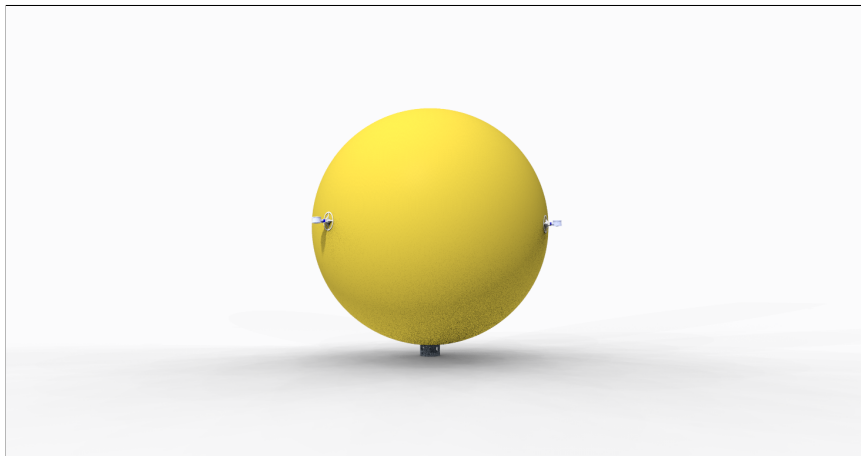

Autonomous Airship Design Executive Summary - GDP 2020



Project Advisors: Dr. Rob Hewson
Prof. Sergei Chernyshenko
Dr. Siti Ros Shamsuddin
Dr. Daqing Yang
Dr. Yongyun Hwang
Dr. Rafael Palacios

Department: Department of Aeronautics
Module: AERO96005 - GDP 2019-2020
Academic Year: 2019/2020

Submission Date: 15/06/2020

Team	Name	Role
FATT01: Configuration Definition	Izaak Caves	Coordination, CAD Environment, Budget and Management
	Easha Tu Razia	Coordination, Remote Control, CAD Environment
	Ming Heng Lim	Coordination, CAD Environment, CAD of Airship Assembly
	Nicole Pellizzon	Coordination, Web App Development, Interactivity
FATT02: Airship Systems	Nikhil Dawda	System Architecture & Hardware Design
	Toby Freeland	System Architecture & Communication Interfacing
	Jeanique C Davis	Hardware Testing & Sensor Data Processing
	Kin Pui Tam	Wireless Charging & Docking Interface
	Sean Chai	2D, 3D Simulation, Mapping, Path Planning & Lidar SLAM
FATT03: Aerodynamics and Propulsion	Elizabeth Lingkan	Power Consumption Analysis, Servo Sizing and Integration, Initial Power Unit Sizing
	Josh Kelly	Buoyancy Factors and Power Consumption, Speed Controller Sizing, Power Distribution Board Selection
	Lewis McDonald	Aerodynamic Forces, Propulsion Layout, Ducted Fan Design and Analysis
	James Anderson	Propulsion System & Battery Sizing, Propulsion System Wiring, Ducted Fan Manufacturing & Testing
FATT04: Structures and Manufacturing	Gael Astier	Envelope Material Selection, Helium permeability, Manufacturing & Assembly
	Constanca Rosas	Gondola Design, Manufacturing & Assembly
	Rhys Van Der Linde	Motor Mount Design, Manufacturing & Assembly
	Nutnicha Saduagkan	Envelope Structural Analysis & Off-Design Structural Performance
FATT05: Flight Dynamics and Control Systems	Jeffrey Yam	Control Development (NPC), Trajectory Shaping, 3D Simulation
	Alexander Popov	Control Development (LSDP), Flight Dynamics, Feedback Linearization
	Bianca Giocas	Control Development (LQR, Integral control)
	Nikhil Purmessur	Control Development (MPC), Signal Processing
FATT06: Payload and Ground Infrastructure	Vy Vo	Subteam Coordination, Visual Odometry
	Ian Lim Ming En	Ground Docking Station
	Tani Afolabi	Visual Obstacle Detection
	Shomik Milki	Ground User Interface

CONTENTS

List of Figures	iv
List of Tables	iv
I Configuration Definition	1
I-A Problem Statement	1
I-B Vehicle Specifications	1
I-C Mission Scenarios	1
II Design Overview	1
II-A Layout	1
II-B Weight Analysis	1
II-C Performance Estimates	1
III Airship Systems	1
III-A System Architecture	1
III-B Hardware Selection	2
IV Aerodynamics & Propulsion	2
IV-A Propulsion System	2
IV-B Thrust Requirements	2
IV-C Ducted Fan Design	2
IV-D Wiring	2
IV-E Propulsion System and Control Integration	2
V Structures	3
V-A Envelope	3
V-A1 Design	3
V-A2 Manufacturing	3
V-B Payload Structural Design	3
V-B1 Motor Mounts' Design	3
V-B2 Gondola Design	3
V-B3 Manufacturing and Adhesives	3
VI Flight Dynamics & Control System	3
VI-A Flight dynamics	3
VI-B Linearised Model	3
VI-C Control System	3
VI-D Trajectory Shaping	3
VI-E Physical Characteristics	3
VII Battery	4
VII-A Power Draw Estimates and Battery Sizing	4
VII-B Autonomous Charging	4
VII-C Charging Station	4
VIII Navigation	4
VIII-A Mapping and Localisation	4
VIII-A1 SLAM	4
VIII-A2 Visual Odometry	4
VIII-B Path-planning	4
VIII-C Obstacle Detection	5
VIII-C1 ToF Sensors	5
VIII-C2 Visual Obstacle Detection	5
IX Interactivity	5
IX-A Operator Interaction	5
IX-B Visitor Interaction	5
X Integration	5
XI Simulation	5
References	6
Appendix A: Additional Mission Scenarios	7
A-A Autonomous Mapping	7
A-B Imperial College Receptionist's Guide	7

Appendix B: Alternative Layout Studies	7
B-A Envelope Shape	7
B-B Motor Configurations	7
B-C Charging Methods	7
Appendix C: Detailed Hardware List	7
Appendix D: Visitor Interactivity Methods	7
D-A Gestures	7
D-B Direct Voice Commands	7
D-C Web application	8
Appendix E: Properties of the Electromagnets	8
Appendix F: Structural Drawing Sheets	9
F-A Motor Mount Diagrams & Drawings	9
F-B Gondola Diagrams & Drawings	10
G Controller Design Considerations	12
H Successful Autonomous Flights on Various Unseen Maps	12

LIST OF FIGURES

1	CAD model of the overall layout of the airship		1
2	System hierarchy and simplified architecture		2
3	Model of ducted fan design		2
4	Structural attachments		3
5	The forces on the airship, excluding drag		3
6	Overall control system		4
7	Charging Method		4
8	MATLAB GUI with output measurements from the airship		5
9	Simulink 3D Animation used for full systems integration.		5
10	Motor configurations considered. See Table IV for associated mass fractions.		7
11	A motor mount assembled with a proximity sensor and a servo		9
12	Gondola base and ring top.		10
13	Autonomous flight in simple map		12
14	Autonomous flight in complex map		12
15	Autonomous flight in Imperial College map		12

LIST OF TABLES

I	Weight breakdown of the components		1
II	Performance Estimates		1
III	Sensor Selection		2
IV	Comparison of different motor configurations based on empirical data for different motors/engines. The motors were sized using an estimate of power draw for 40 minutes of hovering as a basic requirement.		7
V	Hardware Selection		8
VI	Properties of the electromagnet		8

I. CONFIGURATION DEFINITION

A. Problem Statement

Design a small autonomous airship for surveillance inside a known or unknown building with the ability to autonomously navigate and map its surrounding. It should also be able to be used for open days with sufficient interactive features [1].

B. Vehicle Specifications

The airship was designed to be able to perform the following [2]:

- Map an unknown area autonomously (day or night)
- Navigate autonomously (day or night)
- Charge autonomously within 30 minutes
- Fly continuously for at least 30 minutes
- Achieve an operating speed of 1.5 m/s
- Cruise at altitude of ≈ 2 m with an operational ceiling of over 10 m
- Have obstacle detection and avoidance capability
- Interact with people
- Communicate in real-time with the ground station
- Operable in both autonomous and manual control modes

C. Mission Scenarios

An Autonomous mapping mission is detailed in Appendix A which has to run before the following missions if any maps need to be generated. A CAD model of the airship performing an autonomous mapping in a warehouse is shown in Fig. 1. Before a mission begins, the ground station must be set up and calibrated.

Surveillance

The airship serves as a solution to resolve the limitation of blind-spots set by conventional wall-mounted CCTV due to its manoeuvrability. It also has the ability to warn intruders of trespassing with its on-board speaker [3].

- 1) The relevant map is downloaded by the airship.
- 2) The airship manoeuvres randomly, patrolling the area.
- 3) On recognition of a person, it plays a pre-recorded message to warn the intruder they are trespassing.
- 4) The airship updates the ground station that an intruder has been located, while continuing to track them via object tracking, detail in Section VIII.

Open Day Interaction & Navigation

- 1) The relevant map is downloaded by the airship.
- 2) Once localised, it stations itself at the closest waypoint, facing an entrance.
- 3) Upon detecting face(s), a pre-recorded greeting is played, introducing the web app. Web app is detailed in Section IX-B.
- 4) The visitor accesses the web app and requests the airship takes them to a specified waypoint.
- 5) The airship plays a confirmation message and begins navigation journey.
- 6) Upon arrival, the airship plays a goodbye message and returns to the entrance waypoint.
- 7) This continues until there is low battery. Then, it returns to the ground station for autonomous charging.

A similar mission where the Receptionist can control the ground station and the airship for people who don't have any internet devices on them is detailed in Appendix A [3].

II. DESIGN OVERVIEW

A. Layout

The final layout of the airship consists of a spherical envelope with three motors placed equidistantly around the envelope mid-line. The spherical geometry maximises the volume to surface area ratio, permitting a large payload. It also has greater air resistance which is insignificant at the operating speed. Even though the tricopter configuration complicates design and control, it is more efficient for mass and power and has a more flexible directional manoeuvrability.

B. Weight Analysis

For negative bouancy the lift generated by the lighter-than-air Helium gas (He) must be lower than total weight of the airship. Table I shows a breakdown of weight by sub-team.



Fig. 1: CAD model of the overall layout of the airship

TABLE I: Weight breakdown of the components

Sub-team	Component	Mass (g)
Systems	Combined Sensor Mass	51.82
	WiFi Antenna Mass	0.70
	Computer board	8.00
	Misc (support hardware, speaker)	22.64
	Wiring	54.50
Propulsion	Ducted Fan	36.33
	Motor	15.90
	Servo	27.00
	Speed Controller & Dist. Board	9.60
	Connectors	22.00
	Battery	117.00
Structures	Wires	100.73
	Envelope	182.69
	Seams	2.00
	Propeller supports	48.00
	Gondola	61.11
	Valve	18.10
	Total	778.12 g

C. Performance Estimates

The key parameters and performance estimates of the airship have been tabulated below in Table II:

TABLE II: Performance Estimates

Key Parameter	Value
Envelope Diameter	1.1 m
Lifting Gas	He (0.1664 kg/m^3)
Total Buoyancy Lift	735.53 g
Minimum Lift	6.973 N
Minimum Lift Mass	710.81 g
Minimum Endurance	30 minutes
Max % Mass Overshoot Allowed	10%
Target % Mass Overshoot	6%
Maximum Operational Altitude	325 m
Drag Coefficient, C_D	0.40
L_{Buoyancy}/D	13.73
Energy Required	40.3 kJ
Motor Power to Mass ratio	11.84 W/g
Maximum Motor RPM	88800

More mission efficiency parameters can be found in [4].

III. AIRSHIP SYSTEMS

A. System Architecture

A system hierarchy was established to ensure a top-down level of control of the airship. This was done to ensure fail safes and redundancies can be implemented in a logical manner to prevent abnormal system and control behaviour. Fig. 2 shows an overview.

Three possible pathways for sensory data to be processed can be inferred from Fig. 2:

- 1) **Immediate Action Protocols:** A set of specific reference signals that help resolve any particular hazardous situations that the airship could be in. Triggered by interrupt signals from specific sensors.
- 2) **On-board Mapping and Navigation:** Sensor and camera data is passed to a mapping and path finding algorithm which generates a reference signal as an output. The given trajectory planned is checked for its potential power consumption. If it's too power

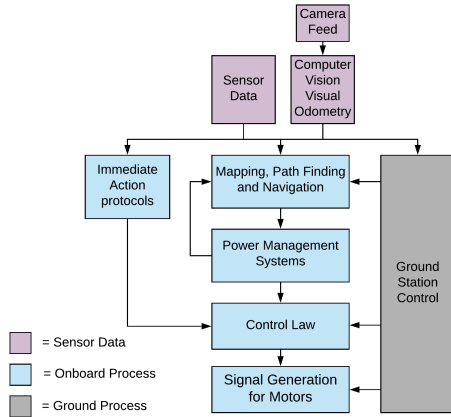


Fig. 2: System hierarchy and simplified architecture

hungry that a safe return to the docking station is unlikely, a new trajectory is requested.

- 3) **Ground Station Control:** The ground station receives a live data feed from the airship. The operator has the ability to take over control authority by either feeding way-points to the path finding algorithm or using a joystick controller to directly control the motors.

A more detailed system architecture can be found in [5].

B. Hardware Selection

TABLE III: Sensor Selection

Sensor	Suitability
Accelerometer/ Magnetometer	Heading angle and acceleration measurements for control
Triple-Axis Gyroscope	To measure angular rates; important for turning and control
Time of Flight Sensor	Obstacle detection and mapping
Pressure w/ Altimeter	Pressure and altitude measurements for control
Current/Voltage	To measure current draw and emf across the battery
Speaker + Amplifier	To interact with people
IR LED	Illuminate camera's FoV with IR in poor visibility conditions such as the dark
Camera (no IR filter)	For Computer Vision and visual odometry for navigation and obstacle detection

Based on the missions defined in Section I-C, the required hardware was identified and selected based on their capability and compatibility with the selected on-board CPU, Raspberry Pi Zero W. Hardware was chosen by minimising a cost function that linked price, power draw and mass. The Raspberry Pi Zero W was chosen for having low form factor, mass and power consumption without much compromise in functionality. Hosting a 1 GHz CPU with 512 MB of RAM alongside a CSI and I2C interface with 40 GPIO pins means we can support and process information from many peripheral devices. Table III contains the list of the key sensor types and camera hardware that are present on the airship.

A detailed component list, including the supporting hardware can be found in Appendix C.

IV. AERODYNAMICS & PROPULSION

A. Propulsion System

The propulsion system was chosen due to its low battery mass fraction and best manoeuvrability. Alternative motor configurations considered can be found in Appendix B-B. The motors are all attached to 180° servos so they may be rotated to provide vertical thrust for altitude control. The initial analysis of the different configurations can be found in [6] which is expanded upon in [7] as better methods for analysing the propulsion system's constituent components were found.

Ducted fans powered by brushless motors were chosen as the method of propulsion. These were sized based on the thrust and endurance requirements, using data from existing ducted fan designs. More information can be found in [6].

B. Thrust Requirements

The limiting thrust requirement was given by required stopping distance. The scenario considered to give the limiting value was:

The airship senses a person moving at a brisk walking speed of 1.8 m/s directly towards it whilst it is moving at the typical cruise velocity (1.5 m/s).

As stated in Table III, time of flight sensors were used for obstacle detection. They were mounted on the surface of the envelope on the motor mounts (see Section V-B1) and considered to have a minimum sensing distance of 1 m [8]. If no action is taken by either party, the airship and the person would collide after 0.303 s when the front of the airship has covered 0.4545 m.

As a basic requirement, the airship should be stationary at the point of collision. This requires a deceleration of 2.475 m/s². Thus, the maximum thrust required from a motor is 1.16 N.

Further details on thrust requirements and collision calculations are given in [7] and [8] respectively.

C. Ducted Fan Design

To minimise mass, the shroud of the ducted fan and the fan blades were 3D printed, which also allowed rapid prototyping development. This also had the benefit that fan blades could be designed and manufactured to satisfy the exact requirement of the mission. To design the fan, blade element theory was used [7]. The manufacturing process is documented in [6].

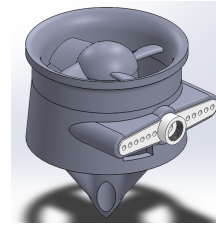


Fig. 3: Model of ducted fan design

The fans have a diameter of 30 mm. The motors were selected based on the requirements of the fan [6]. For the duct to provide a benefit to the thrust to power ratio of the fan when compared to an open propeller, it's mass must be less than 6.53 g. The mass of the ducted fan components are 6.39 g, 3.99 g and 1.73 g for the duct, motor mount and fan respectively. For a more in depth analysis of the ducted fan design see [7].

An experiment was set up to test the operation of the ducted fan units. Issues were found with forces due to an imperfectly balanced fan and led to updates in the ducted fan design [6, 7].

D. Wiring

Flexible wires were selected to connect components along the sides of the envelope to allow the airship to be inflated and deflated without needing to remove them. Where wires entered the gondola, connectors were used to allow easy removal and maintenance of the gondola and the components within. The battery also used connectors, should it need replacing. The propulsion system wiring was discussed in more detail in [6].

E. Propulsion System and Control Integration

The input response of each element of the propulsion system was required so that the Controls team could design a control system that would send the correct signals to each component. Using the DSHOT protocol the speed controllers could set the motors to specific rotational velocities [9]. The expected performance of the ducted fan could then be calculated using the analysis carried out in [7]. The response of the servos to different PWM signals was also found [10]. A summary of the control and propulsion system has been provided in [6].

V. STRUCTURES

A. Envelope

1) *Design:* The envelope consists of a super-pressure balloon made of a single 48 μm layer of TPU (thermoplastic polyurethane).

The internal pressure required for minimal deflection at motor mounts was found to be approximately 875 Pa. At this pressure, the maximum hoop and longitudinal stress occurs at the top of the envelope with values 5.16 MPa and 5.00 MPa, respectively. The selected material was found to be sufficient in withstanding stresses across the envelope including the seams and payload attachments even with an included safety factor of 4 in accordance with the FAA non-rigid Airship structural design criteria.

The internal pressure also deforms the envelope with a 10.12% strain, meaning a 1.00 m pre-inflation diameter is sufficient to expand to the required 1.10 m diameter. More information on the calculations and design process to reach these values can be found in [11].

Special attention has been paid to the He permeability characteristics of the envelope, with the design objective of reducing daily volume loss to under 1% and a predicted value of 0.1% without including the effect of potential defects [12]. An analysis of the consequences of said defects on the ability to complete the mission has also been conducted and a limiting case of 4 pinholes (0.1 mm hole) corresponding to a 6% net daily lift loss was identified as the point when replacement of part of the membrane would be necessary [11]. The valve system used is an 18.1 g PVC screw valve for easy inflation and deflation [12]. It is located at the bottom of envelope, where there are minimum He losses.

2) *Manufacturing:* The TPU membrane is bought to specifications of 2 m width and 48 μm thickness as a roll of already cast-extruded material made from powder form. The 3D spherical shape is obtained by heat bonding of the thermoplastic inside a hemispherical mould, taking advantage of the thermal and physical properties of the elastomer for strong and easy jointing. The valve is integrated to the membrane using the same adhesive and primer as used for the motor mounts. More information regarding the manufacturing process can be found in [12].

B. Payload Structural Design

1) *Motor Mounts' Design:* The motors are attached to the envelope via 3 equidistant motor mounts which are attached to the middle of envelope via adhesives to ensure a statically determinate structure, with minimal mass as shown in Fig. 4a. Each motor mount will support a proximity sensor and a servo, bound to the motor mount using two M2x8 screw with helicoils to reinforce the thread, atop which the ducted fan and motor will sit. By itself, the motor mount weighs up to 10.15 g and has a base of radius 40 mm to prevent the envelope skin and motor mount rotating more than 1° which could cause excessive deformations. Full dimensions and drawings can be found in Appendix F-B and more information in [13].



Fig. 4: Structural attachments

2) *Gondola Design:* A gondola base is screwed to a ring structure attached to the bottom of the envelope via adhesives as shown in Fig. 4b. The 3 mm screws allow the gondola to be detached for maintenance purposes. Full dimensions and drawings can be found in Appendix F-B and more detail can be found in [14].

3) *Manufacturing and Adhesives:* The gondola and fan motor mounts are 3D printed using Fused Deposition Modelling (FDM). A thermoplastic specifically designed for 3D printing is used called ABS M30 which has been synthesised to have superior tensile and layer bonding properties when compared to regular ABS.

TPU is notoriously difficult to bond to due to its low surface energy, however, Loctite 401 is proven to provide a strong but flexible bond between ABS and TPU, especially when used with Loctite SF770 primer.

VI. FLIGHT DYNAMICS & CONTROL SYSTEM

A. Flight dynamics

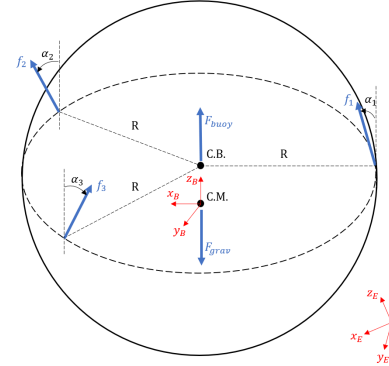


Fig. 5: The forces on the airship, excluding drag

The flight dynamics equations were derived by considering the behaviour of a tricopter with the buoyancy and drag effects of the envelope. The resulting model is shown in Fig. 5.

B. Linearised Model

Controller design was based on two linearised models of the physical dynamics, one using Feedback Linearisation and another using Robust Feedback Linearisation. Both give exact linearisations via input transformations within the system architecture. The latter has the advantage of being less sensitive to model uncertainty, but it adds complexity to the design process.

C. Control System

The primary objective of the control system is to ensure that the airship follows the path set in the navigation algorithms. This is achieved by minimising the error between the desired path and the current path, and using a controller to determine the changes to the propeller thrust and motor tilt angles that will minimise this difference. Fig. 6 shows the structure of the control system. A comprehensive description on the considerations that goes into the controller's design can be found in Appendix G.

D. Trajectory Shaping

Any control system will struggle to follow a trajectory if the path is defined with a series of abrupt commands. To refine the control performance, the desired path is translated into a versatile set of reference signals, calculated so as to produce the most efficient path between two waypoints. This technique accounts for the physics of the system and the limitations in the motors, thus creating a trajectory which suppresses any unnecessary actuator adjustments.

E. Physical Characteristics

According to the simulations on the control system, the airship's operational speed is limited by the weight excess and the complexity of the path. When flying on a straight trajectory, it can comfortably maintain the target upper bound speed of 1.5 m/s. To avoid excessive pitching, this speed can be reached with an initial 'jerk' from 0 to 0.5 m/s, followed by a more gradual acceleration over 10-20 seconds. When turning, the airship must stay below 1 m/s to avoid rolling. Trajectory shaping can greatly improve the performance in vertical ascent and descent, thus providing good control in takeoff and landing stages.

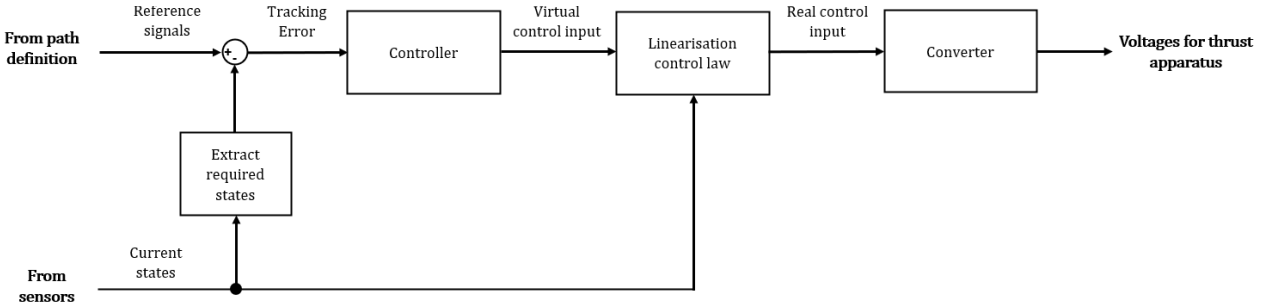


Fig. 6: Overall control system

VII. BATTERY

A. Power Draw Estimates and Battery Sizing

To ensure the airship is able to complete the mission profile, the battery needed to be able to provide a total power of 40.3 kJ (including transmission losses) before requiring recharging. The power consumption of the different mission phases was updated and crosschecked by all members of the Propulsion and Aerodynamics team. 24.6 kJ was needed by the propulsion system and 15.7 kJ was needed to power the other onboard systems. A 11.1 V, 1500 mAh LiPo battery was selected to meet the power requirements and to be able to supply the correct voltage to the motors [6]. Detailed power draw estimates for different flying scenarios are given in [10].

B. Autonomous Charging

Autonomous charging is done using pogo pins. The minimum time to fully charge is 16 minutes at 5 A with power of 10 W using magnetic induction. Alternative charging methods are discussed in Appendix B-C.

Pogo pins allow the battery to charge in any arbitrary heading direction. When the airship returns to the proximity of the dock, it is able to descend onto the charger with the use of docking markers, as described in Section VII-C. To achieve this, the pogo pins are connected in parallel and are placed on the circumference of the charger, with a ground pin in the centre to complete the circuit. A slotted ring is attached to the bottom of the gondola in order to collect current from the pogo pins.

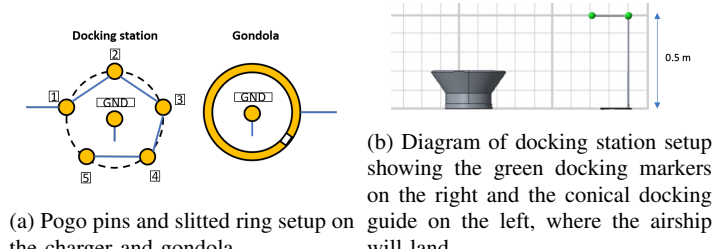


Fig. 7: Charging Method

Pogo pins are sprung conductors and have a stated working travel for lowest resistance tested out by the manufacturer. Since our airship is designed to be slightly negatively buoyant, two electromagnets connected in series are used to provide moment-balanced downforce to the airship, required to compress the pogo pins to their working travel.

C. Charging Station

Referring to Fig. 7b, the docking station is composed of two key pieces of hardware: the docking markers and the conical docking guide.

As the airship approaches the docking station, it uses the docking markers to align itself. Colour detection is used to position the airship relative to the docking station, using the docking markers. This requires pre-flight calibration. The use of three spherical blob markers spaced as points of a triangle are used to give the airship an altitude reference. The docking markers are designed to be portable and easy to setup with a small footprint.

During the docking procedure, the standard control system is overridden with a control system designed specifically for this procedure. It would require calibrating to measure output error which is subsequently removed through feedback.

The final part of the docking procedure is ensuring the alignment of the pogo pins for charging. This requires a very high level of accuracy that is difficult to achieve using motor control alone. As such, a more appropriate mechanical solution was chosen. The airship enters the docking guide through a wide mouth. As it loses altitude, the conical shape of the guide controls the position of the airship in the x - y plane.

VIII. NAVIGATION

The Navigation toolbox in MATLAB was exploited for its Simultaneous Localisation and Mapping (SLAM) map builder, path planning using Rapidly-Exploring Random Tree Star (RRT*) algorithm and sensor modelling. The Computer Vision and Image Processing toolboxes in MATLAB were used for processing visuals from the onboard camera for navigation.

A. Mapping and Localisation

1) *SLAM*: Pose estimation and localisation is currently conducted via visual-SLAM with current developments being made to fuse data from inertial, visual and ToF sensors to generate an accurate pose estimate. This is proposed to be done via an initial estimate generated by a state estimator with the accelerometer and gyroscope data as inputs followed by SLAM localisation via vision and finally refinement via drift correction using ToF sensors [15].

2) *Visual Odometry*: This method is useful in conjunction when executing SLAM with time of flight (ToF) sensors as pure ToF maps drift due to accumulated errors. Visual odometry allows the airship to localise itself relative to its starting position through visual inputs (camera feeds). An indirect method of visual odometry has been implemented (feature-detection approach) as direct methods are too computationally taxing on the system. An ill-posed problem with visual odometry is scale uncertainty. From the solutions explored, it was concluded that combining with inertial measurements provides the accurate absolute localisation required for general localisation and integration into SLAM. However, fusion of visual, ToF and inertial sensors has complexity beyond the scope of this project and would be carried out in future developments. Full details of the application of visual odometry in this project is given in [16].

B. Path-planning

Path-planning is done with the goal of reaching a goal pose without colliding with an obstacle. We used a rapidly-exploring random tree star (RRT*) algorithm to achieve this. This algorithm was chosen for the relatively smooth paths it produced. With increased knowledge of the operating environment (eg. with manual flight) the path planned becomes more ‘optimised’, requiring less u-turns as it plans for the shortest possible path to the goal with the onboard map of the mapped world around it. This gets updated every time new obstacles, are added detected and to the map. A new set of waypoints are the generated by the algorithm for the airship to follow [15].

C. Obstacle Detection

1) *ToF Sensors* : The airship also uses the ToF sensors to detect obstacles that come close to the airship. This data is continuously fed into the generated map and used for path planning. If these obstacles continue to move closer to the airship, past a certain threshold, an emergency stop procedure is initiated to prevent collision.

2) *Visual Obstacle Detection*: Computer Vision toolbox in MATLAB contains pre-trained models with optimised feature detection of faces, pedestrians and other common objects in images and videos which made implementation easy. For specific feature detection, machine learning algorithm are implemented, which require a large data set to train, and as a result are expected to get better with time.

IX. INTERACTIVITY

A. Operator Interaction

An operator is a student or member of staff who has a thorough understanding of the airship's systems and capabilities and will be supervising the airship's flight. This type of interaction is required for initial testing, emergency manual override and monitoring.

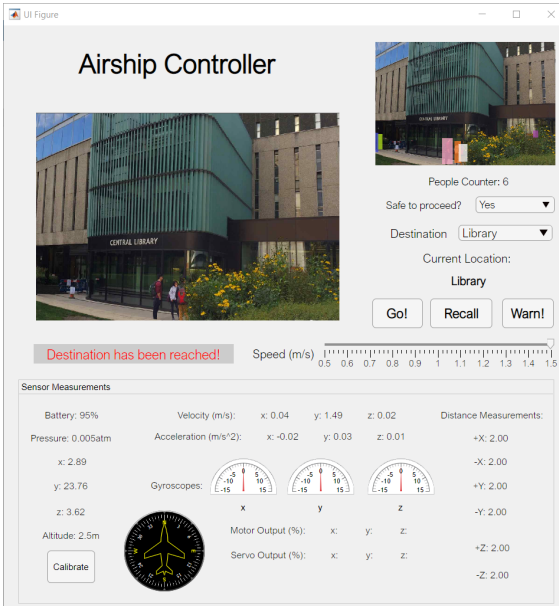


Fig. 8: MATLAB GUI with output measurements from the airship.

To accommodate this, a MATLAB graphical user interface (GUI) was created. As can be seen in Fig. 8, the GUI features a live video stream from the airship's on board camera and is also used to calibrate the airship after takeoff. It also displays current way-point navigation map. Manual control uses a remote controller (such as a PS2 controller) plugged in.

B. Visitor Interaction

Visitor interaction is a key component of several missions such as an Open Day scenario. See Appendix D and [8] for a full discussion on interactivity options investigated. A web app was chosen as the medium for visitor interaction, capitalising on the 88% of people aged 18 to 75 that have ready access to a smartphone based on a 2019 UK study [17, pg. 5]. A web app is hosted on a web server and is accessed by the user through a web browser on any internet connected device in the same way as a website.

The final web app has the following functionalities:

- Voice Command - request the airship to perform a pre-programmed flight manoeuvre such as a figure of eight
- Remote Control - control the airship for 10 seconds using two virtual joysticks.
- Destination Request - request the airship navigate to a pre-defined way-point from its current position
- Report - report any issues spotted with the airship

Additionally, there is a detailed Help page to aid users and an Information page with an account of the project.

Each of the individual functionalities are controlled at the ground station. For example, at an Open Day event, only Destination Request is set as active so that the airship can focus on helping visitors navigate the department.

The web app stores data inputs from the user in a cloud-hosted noSQL database hosted on Google's Firebase platform [8].

X. INTEGRATION

The ground station is the communication hub of the overall system. All communication with the airship is handled here. This decision was made to reduce the possibility of the airship receiving conflicting commands as there are multiple input sources and provide some processing assistance. The ground station communicates with the airship over the local WiFi network using an on board antenna to significantly extend the WiFi range of the Raspberry Pi Zero W to approximately 100m. The ground station itself communicates to the ground station using the computer's in-built WiFi therefore limiting the range to being closer to a WiFi AP.

Inputs are received from the MATLAB graphic user interface (GUI) hosted on the ground station computer and from the visitors' web app. Inputs from the GUI are directly fed into the Simulink integration model. Inputs from the web app are sent to an online database. They are then fetched by the Simulink integration model using custom MATLAB function blocks [8].

XI. SIMULATION

3D simulation was done using Simulink® 3D Animation™. As all subteams worked in MATLAB, and the integration was done via a Simulink model, a MATLAB hosted simulation was the most suitable choice. The simulation featured ToF sensors which was used for testing path planning as well as a video camera output which was linked with Computer Vision to test feature detection. Within the Simulink model itself, it allowed for easily replace Simulink blocks to test the overall integration and system hierarchies. While initial testing was completed with the ToF sensors and path planning, subsequent testing of other components such as vision and control law implementation have yet to be conducted due to time constraints.

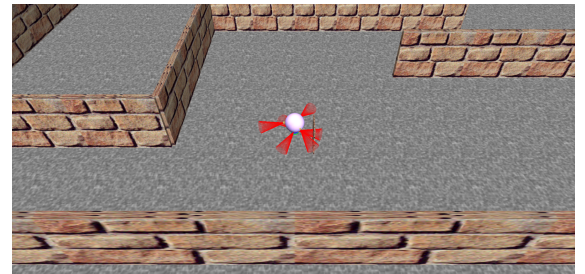


Fig. 9: Simulink 3D Animation used for full systems integration.

REFERENCES

- [1] R. Hewson. 3rd-year group design project statement. 2020.
- [2] Izaak Caves. Autonomous airship design individual report - configuration definition. Technical report, Department of Aeronautics, Imperial College London, 2020.
- [3] Ming Heng Lim. Autonomous airship design individual report - configuration definition. Technical report, Department of Aeronautics, Imperial College London, 2020.
- [4] Easha Tu Razia. Autonomous airship design individual report -configuration definition. Technical report, Department of Aeronautics, Imperial College London, 2020.
- [5] Nikhil Dawda. Autonomous airship design individual report - airship systems. Technical report, Department of Aeronautics, Imperial College London, 2020.
- [6] James Anderson. Autonomous airship design individual report - aerodynamics and propulsion. Technical report, Department of Aeronautics, Imperial College London, 2020.
- [7] Lewis McDonald. Autonomous airship design individual report - aerodynamics and propulsion. Technical report, Department of Aeronautics, Imperial College London, 2020.
- [8] Nicole Pellizzon. Autonomous airship design individual report - configuration definition. Technical report, Department of Aeronautics, Imperial College London, 2020.
- [9] Josh Kelly. Autonomous airship design individual report - aerodynamics and propulsion. Technical report, Department of Aeronautics, Imperial College London, 2020.
- [10] Elizabeth Lingkan. Autonomous airship design individual report - aerodynamics and propulsion. Technical report, Department of Aeronautics, Imperial College London, 2020.
- [11] Nutnicha Saduagkan. Autonomous airship design individual report - structural design and manufacturing. Technical report, Department of Aeronautics, Imperial College London, 2020.
- [12] Gael Astier. Autonomous airship design individual report - structural design and manufacturing. Technical report, Department of Aeronautics, Imperial College London, 2020.
- [13] Rhys van der Linde. Autonomous airship design individual report - structural design and manufacturing. Technical report, Department of Aeronautics, Imperial College London, 2020.
- [14] Constanca Barreto Oliveira Da Silva Rosas. Autonomous airship design individual report - structural design and manufacturing. Technical report, Department of Aeronautics, Imperial College London, 2020.
- [15] Sean Chai. Autonomous airship design individual report - airship systems. Technical report, Department of Aeronautics, Imperial College London, 2020.
- [16] Vy H T Vo. Autonomous airship design individual report - payload and ground infrastructure. Technical report, Department of Aeronautics, Imperial College London, 2020.
- [17] P. Lee and C. Calugar-Pop. Global mobile consumer survey: Uk cut. plateauing at the peak. the state of the smartphone. 2019.
- [18] Bombay Indian Institute of Technology. Studies on optimum shapes of envelopes for aerostats and airship. 2004.
- [19] Kin Pui Tam. Autonomous airship design individual report - airship systems. Technical report, Department of Aeronautics, Imperial College London, 2020.

APPENDIX A ADDITIONAL MISSION SCENARIOS

The following 2 missions are also considered throughout the project decisions.

A. Autonomous Mapping

- 1) Initialise autonomous mapping function.
- 2) Airship powers up and climbs to the room's ceiling to gauge the height of the room.
- 3) Begin analysing its surroundings with on-board depth sensors and camera.
- 4) Both navigation systems output a 3D map that constantly overlay each other to remove temporary obstacles, detailed in Section VIII-A.
- 5) As the depth sensor has a range of 80-260 cm, the airship will have to make periodic vertical descents of 80-260 cm each time after making its round around the area.
- 6) After descending to the ground and mapping all accessible areas, the mapping mission is complete. It returns to the ground station for autonomous recharge.
- 7) In the event that the airship has low battery during the mission, it will return to the ground station for autonomous recharge. It then continues the mission where it left off.

B. Imperial College Receptionist's Guide

For this mission, the airship and ground station are explicitly stationed at the reception for the receptionist's usage for normal day's operation.

- 1) A new visitor arrives at the reception and seeks directions to a specific room/location. They do not have a mobile phone with them to directly connect to the airship.
- 2) As the receptionist(s) is unable to leave their post to take the visitor to the location, they will make a navigation request through the airship to the place of interest and request the visitor to follow it.
- 3) During the mission, the receptionist is able to monitor the location of the airship via the on-board camera feed on the MATLAB ground station GUI. They may broadcast any relevant information via the airship's on-board speaker.
- 4) When the airship has reached its destination, it will play a pre-recorded message to notify the visitor of arrival and bid farewell.
- 5) The airship will then return to the reception desk, awaiting further requests, until battery levels reach the recharge point.

APPENDIX B ALTERNATIVE LAYOUT STUDIES

A. Envelope Shape

Initially, a GNVR shape was chosen for the envelope design as it provides a high lift to drag ratio, excellent control and good drag characteristics.[18] However, the requirement of indoor usage of the airship imposes a size constraint and such shape may encounter difficulties steering through tight corners without giving sufficient mass margins. Hence, it was omitted.

B. Motor Configurations

Several motor configurations were considered ranging from two to four motors. These can be seen in Fig. 10.

Key factors of consideration were mass fraction and manoeuvrability. It was decided to use design number 1 for two main reasons.

Firstly, as can be seen from Table IV, the battery mass fraction is one of the lowest, only beaten by design number 5. This means the design has a very good power efficiency.

Secondly, compared to designs 2, 3 and 4, this design has better manoeuvrability. It is able to move in any direction which is desirable for narrow corridors and tight corners.

Unfortunately this design does have the second highest motor mass fraction which is because the fans have the largest thrust requirement due to the orientation of the fans thrust vector not being inline with the direction of motion, which requires larger fans. However, given the other considerations, this was deemed to be a suitable compromise.

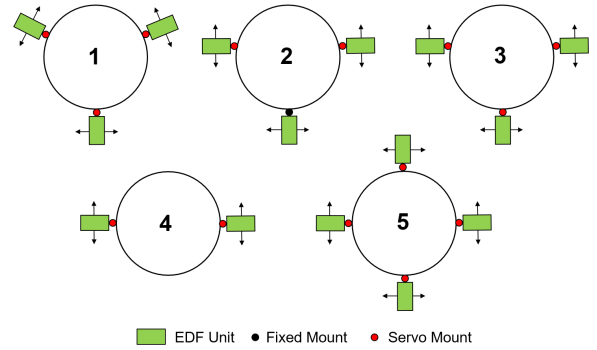


Fig. 10: Motor configurations considered. See Table IV for associated mass fractions.

TABLE IV: Comparison of different motor configurations based on empirical data for different motors/engines. The motors were sized using an estimate of power draw for 40 minutes of hovering as a basic requirement.

Design no.	Mass Fractions		
	Motor	Battery	Total
1	0.0723	0.0265	0.0988
2	0.0589	0.0340	0.0929
3	0.0610	0.0277	0.0887
4	0.0407	0.0340	0.0747
5	0.0787	0.0247	0.1034

C. Charging Methods

One of the requirements stipulated in [1] was "automatic charging". Initially, Qi-standard wireless charging was considered. Limitations in commercial charging pads would have resulted in long charging times of 100 minutes which exceeds the turnover rate requirement of 30 minutes. The choice of a LiPo battery also necessitates cell balancing. This would have required adding a power receiver and a balance charge battery management system to the on board system with the associated mass penalty of up to 20 g. For these various reasons, wireless charging was deemed unsuitable for the task.

A balance charger requires 63 W to fully charge in 16 minutes at 5 A as compared to 10 W required by magnetic induction.

APPENDIX C DETAILED HARDWARE LIST

The selection of hardware was based on functionality, mass, power draw, cost and form factor. For a detailed justification of why the particular hardware in V was chosen, please refer to individual reports from FATT02 and FATT03 [5];

APPENDIX D VISITOR INTERACTIVITY METHODS

A. Gestures

The notion behind this idea is to allow the visitor to directly command the airship through simple gestures where the airship mimics them to a certain extent. This creates a form of personal and dramatic interaction similar to that popularised by the movie "Real Steel".

The use of gestures as a form of interaction requires complex computer vision algorithm to detect said gestures and associate them to corresponding reactions. This also imposes a hefty computational cost on the airship in which at the current state of the project, is deemed not feasible. In addition, such interaction is usually done 1-to-1. As such, when a crowd performs a mix of prefixed gestures, the airship will be unable react accordingly as it gets confused by the amount of multiple inputs.

B. Direct Voice Commands

In order to allow the visitors to verbally commands the airship directly, a microphone is required. In the context of mounting the microphone

TABLE V: Hardware Selection

Hardware	QTY	Purpose
Raspberry Pi Zero W	1	On-board CPU
2.4GHz Mini Flexible WiFi Antenna with uFL Connector	1	To extend range of WiFi connectivity
Adafruit LSM303AGR Accelerometer Magnetometer	1	Heading angle and acceleration measurements
Adafruit L3GD20H Triple-Axis Gyro	1	To measure angular rates of the airship
VL53L1X Time of Flight Sensor	8	Obstacle detection and mapping
Adafruit 1893 MPL3115A2 Precision Pressure Sensor with Altimetry	1	Pressure and altitude measurements
Adafruit INA219B Current Sensor	1	Monitor battery current draw and EMF
Adafruit STEMMA Speaker - Plug and Play Audio Amplifier	1	Speaker for interaction with students
Super-bright 5mm IR LED, Everlight IR33-A	2	Illuminate camera field of vision with infrared
Raspberry Pi PiNoir Camera	1	IR Camera
Adafruit TCA9548A I2C Multiplexer	1	Provides individual I2C addresses to identical sensors
10kΩ Resistors	3	For pull-up resistor configuration on any possible floating logic-gate setups
100kΩ Resistors		
10μF 50V Capacitor		Account for voltage ripples effects
0.1μF Ceramic Capacitors	1	
3.3V 800mA Linear Voltage regulator	1	Voltage Regulator
750Ω E48 resistor	2	current regulation for the NPN transistor and LED.
15Ω E24 resistor	2	current regulation for the NPN transistor and LED.
200mA NPN transistor	2	current control for the LED
Mini Solderless Breadboard	2	Connection Platform for sensors
iFlight XING Nano 1204 2-4S Brushless Motor 6500 kV	3	Motor
20A DYS XSD20A BLHELI-S Dshot 3-4S OPTO Electronic Speed Controller	3	Electronic Speed Controller
SG90 Micro Servo	3	Servo motor for thrust vectoring
Matek Mini Power Distribution Board	1	Splits the power supply from the battery to the motors and on board systems
Turnigy Nano-Tech 1500mAh 3S 30C Lipo(E-flite Compatible EFLB15003S)	1	Provides power to all components listed above
Turnigy Accucel-6 80W 10A Balance Charger	1	To balance charge the battery (not part of the payload)

in the gondola of the airship, a potential problem was realised, such that the ambient noises could saturate the input frequencies of said commands, resulting in an inaccurate Natural Language Processing (NLP). In addition, the airship will be unable to log a queue of voice commands directed at it when multiple visitors try to command it at one go. Lastly, as the airship is designed mainly for autonomous mapping, a microphone serves no useful purpose for such mission hence it will be a dead weight being carried around. Thus, the idea of mounting a microphone on the airship's gondola directly was omitted.

To resolve the issue with input frequencies saturation due to noises, a potential solution was to have a coiled microphone uncoil down from the airship's gondola that allows a visitor to directly give verbal commands to the airship. This also resolves the issue of logging the queue for such interaction inputs. However, said solution imposes additional weight due to the extensive length of wires and a coiling mechanism to be installed which will be redundant during the autonomous mapping mission. Finally, in the event that a visitor tugged the microphone too strongly, the airship dynamics and control system will be greatly affected, imposing direct instability. Hence, the idea was scrapped.

Furthermore, it was realised that with verbal commands, there could be issues with accents leading to inaccuracy of interpretation. Hence, necessitating another method of interaction with the airship.

C. Web application

The resulting solution is then to have a web-application that anyone with a device connected to the internet can easily access - by scanning a QR code or typing in the shorten URL of the web-application into their web-browser. This greatly removes the hassle of installing a mobile-application solely for interaction purposes. In addition, the web-application can be configured to accept multiple inputs in the form of text, voice and pre-configured selection of options hence having a great amount of flexibility. Furthermore, the implications stipulated in other methods are easily resolved in this mode of interaction - no additional weight imposed, minimal ambient noises when using individual device's microphone, logging a queue for inputs can be done systematically and there are no direct implications to airship dynamics and controls.

APPENDIX E

PROPERTIES OF THE ELECTROMAGNETS

The following table shows the calculations and properties of the electromagnets within the docking station. Note that the table provides the properties of one of the two identical electromagnets connected in series. Permeability of free space $\mu_0 = 4\pi \times 10^{-7}$ kgm/(As)². The installation of the pogo pins and the design of the electromagnets are fully explained in [19].

TABLE VI: Properties of the electromagnet

Parameter	Unit	Equation	Value
Wire diameter D_w	mm		0.664
No. of turns N			35
Iron core length L_b	mm	$D_w N$	23.2
Iron core diameter D_b	mm		30
Iron core area A	mm ²	$\pi D_w^2 / 4$	706.86
Current I	A	V_s / R	0.332
Distance from magnet to metal G	mm		0.1
Turns per layer T		L_b / D_w	35
No. of layers W		N / T	1
Overall radius r_w	mm	$WD_w + D_b / 2$	15.7
Overall area A_0	mm ²	πr_w^2	770.82
Inductance L	μH	$\frac{\mu_0 N^2 A}{L_b}$	2.68
Force F	N	$\frac{(NI)^2 \mu_0 A}{2G^2}$	5.98

APPENDIX F
STRUCTURAL DRAWING SHEETS

A. Motor Mount Diagrams & Drawings

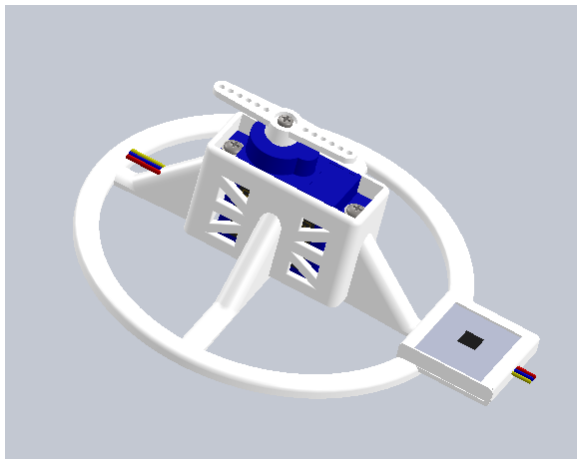
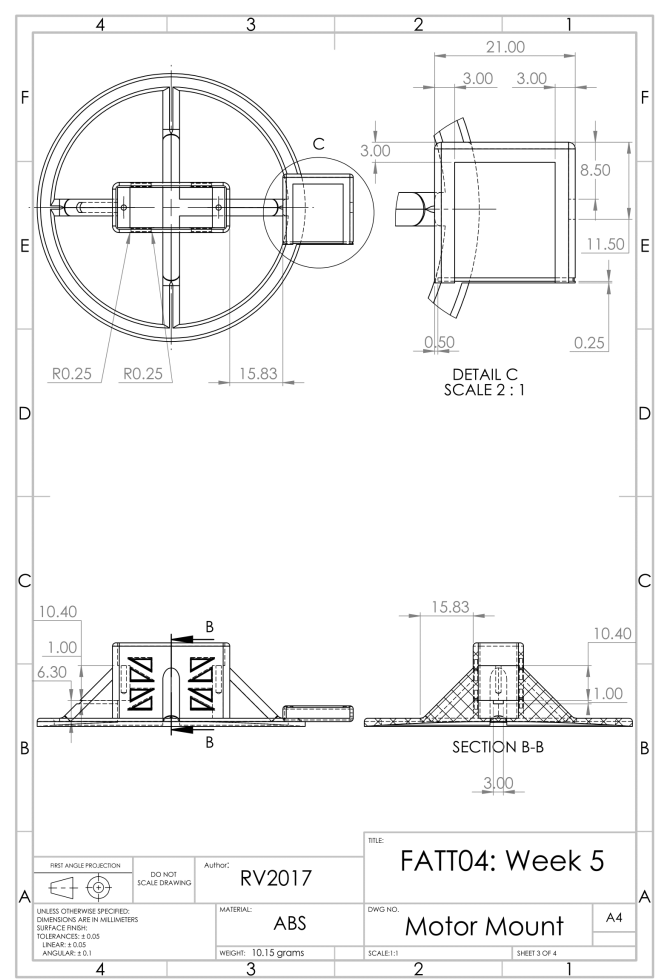
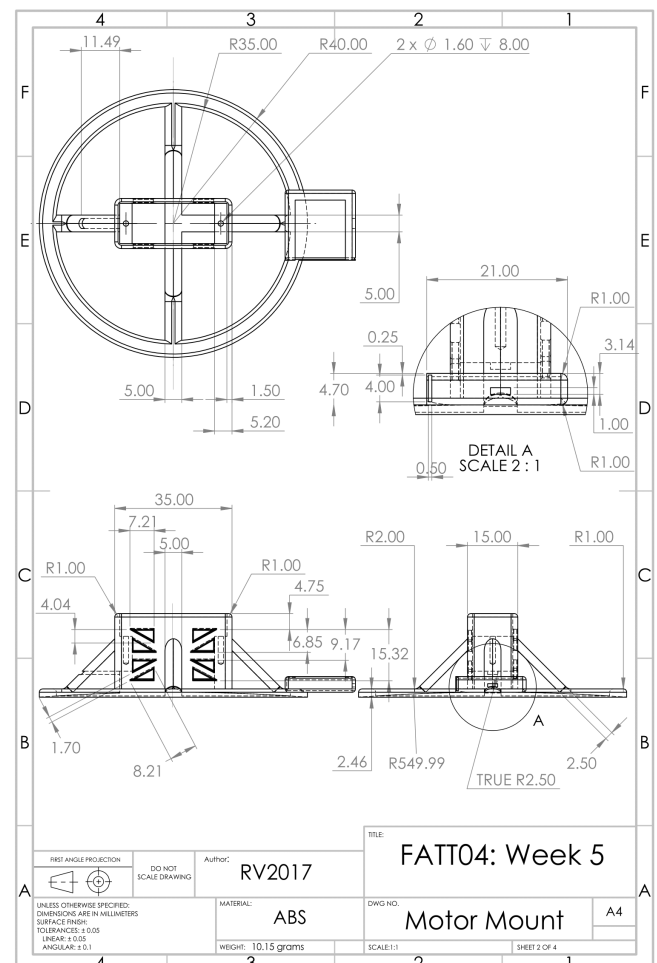
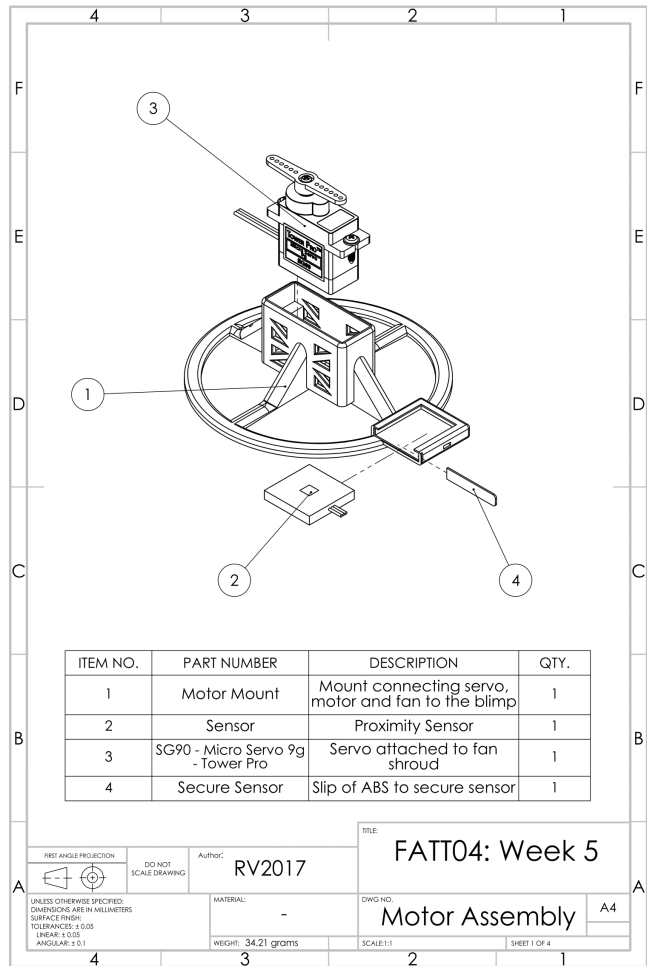
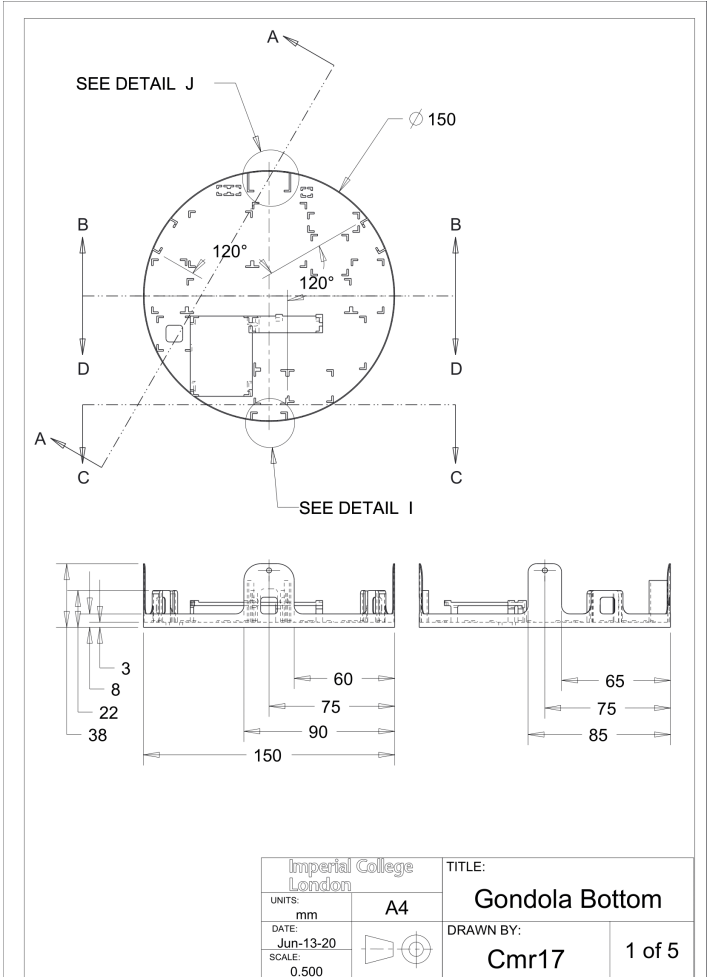
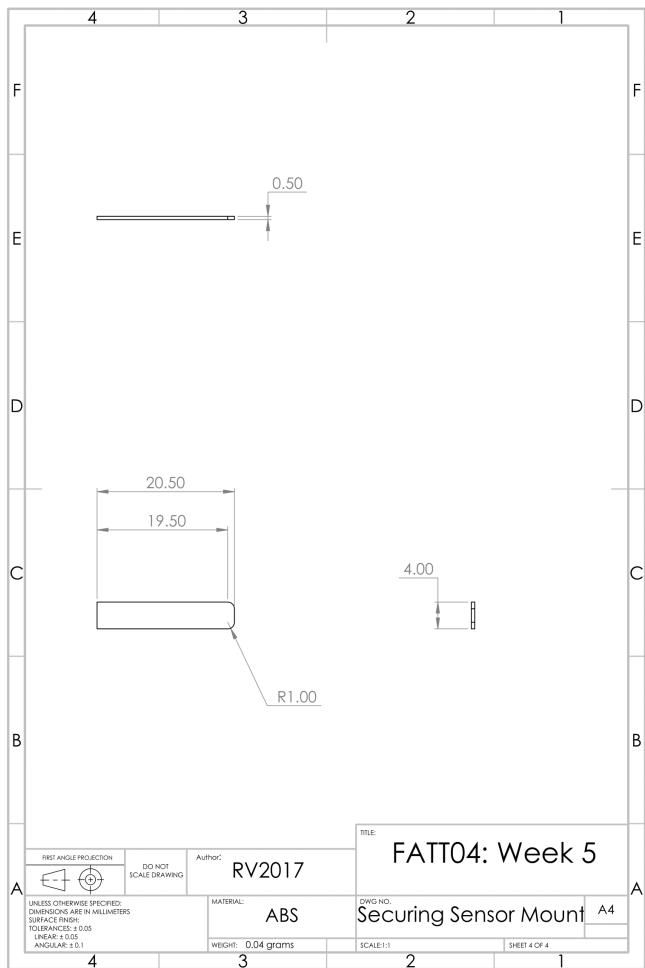


Fig. 11: A motor mount assembled with a proximity sensor and a servo

Drawing sheets for the motor mount:





B. Gondola Diagrams & Drawings

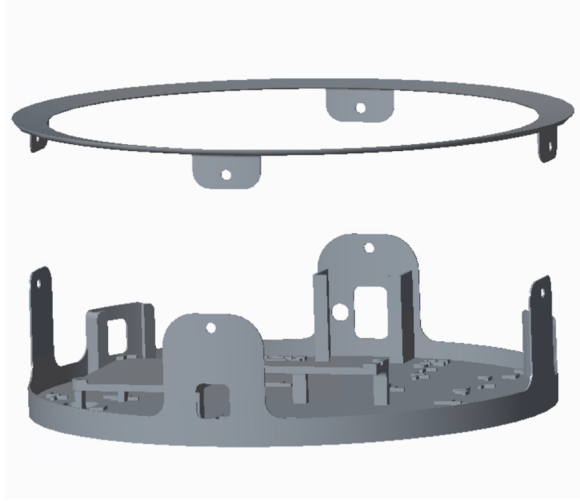
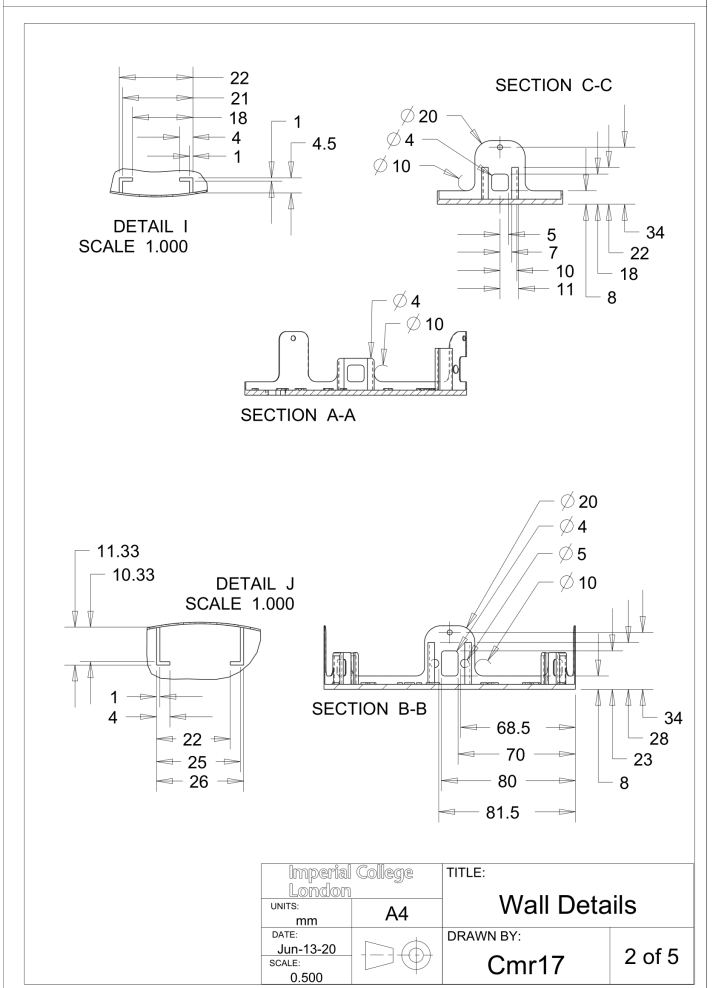
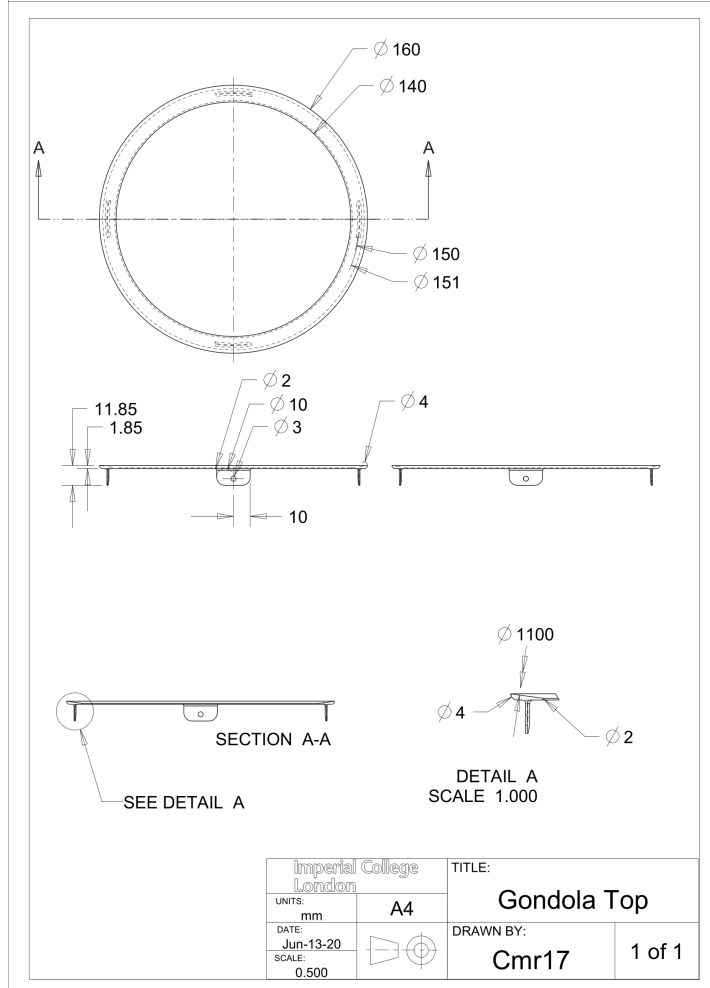
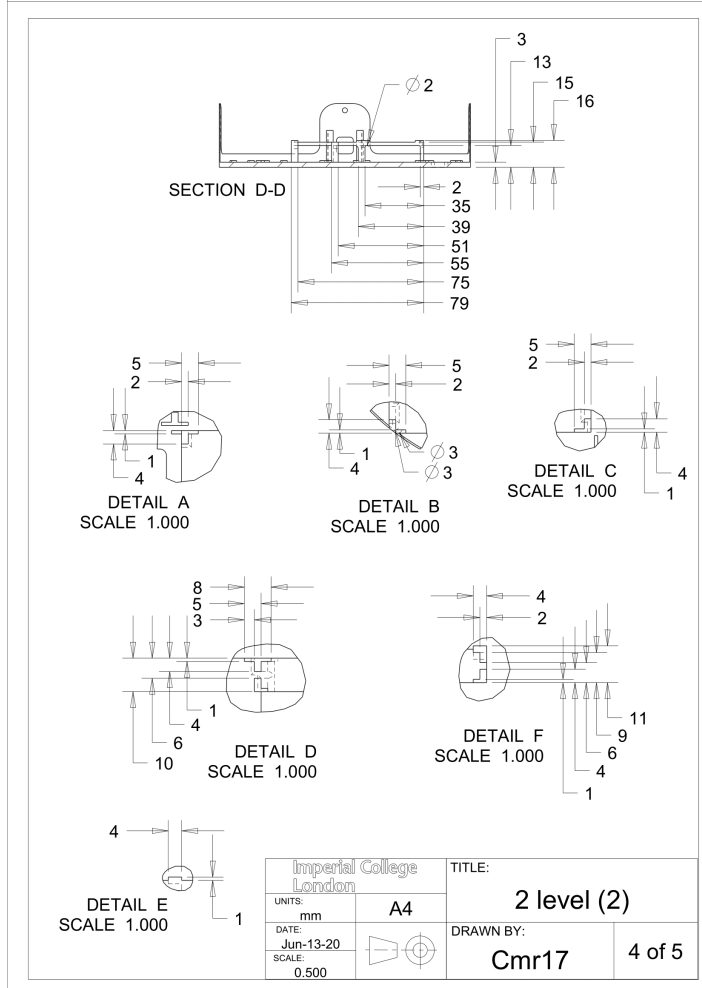
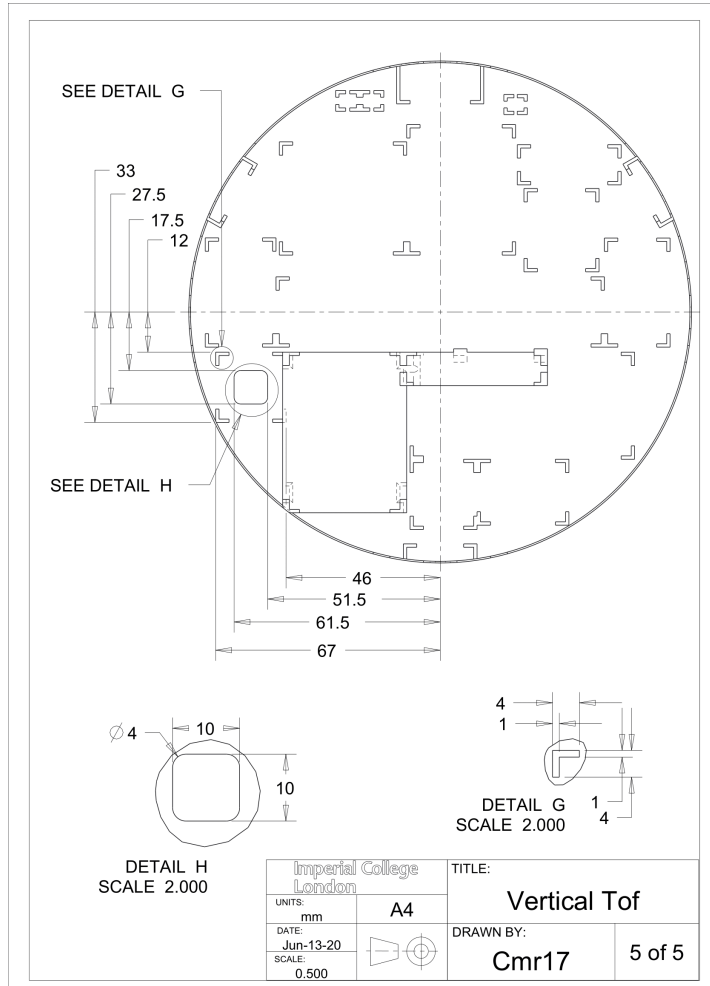
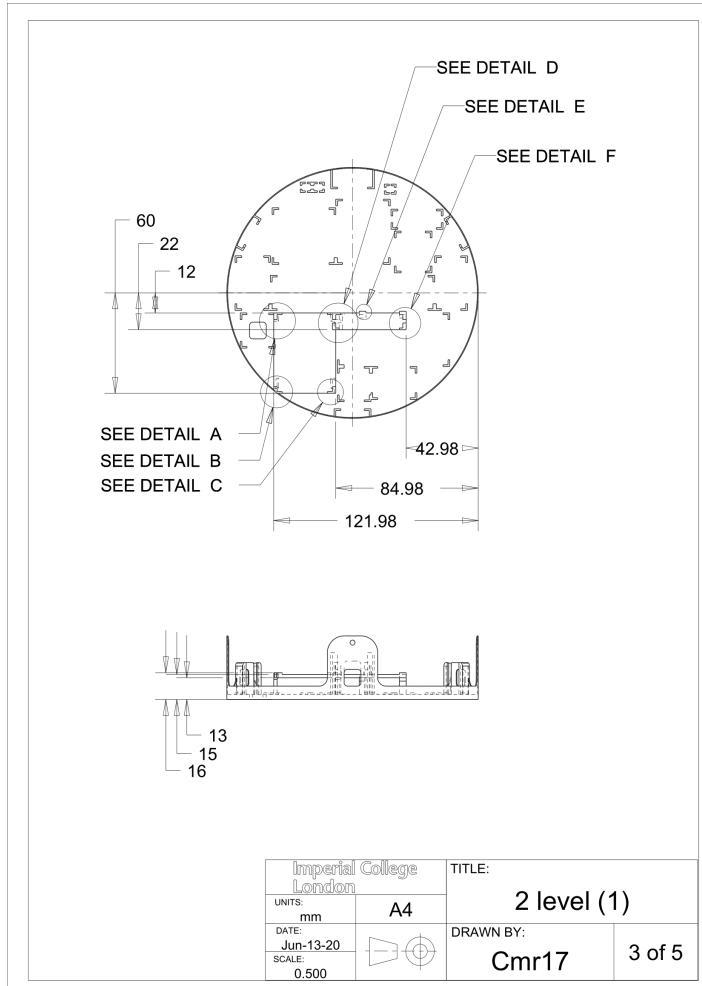


Fig. 12: Gondola base and ring top.





G CONTROLLER DESIGN CONSIDERATIONS

Initially, four control design methods were considered: Model Predictive Control (MPC), Linear Quadratic Regulator (LQR), H_∞ Loop Shaping Design Procedure (LSDP), and Neural Predictive Control (NPC). The latter can be applied to the nonlinear system, whereas the other three use the linearised models. As well as good tracking of a desired trajectory, the designs are evaluated by the following criteria: the controller should achieve steady state values with an efficient route which does not require large actuator expense; the tracking error performance should not worsen for more complex reference signals, such as turns and sudden stops; the controller should be robust, meaning that it is as valid in the real system as it is in the linearised model, despite the uncertainties in the latter; the controller should attenuate load disturbances (e.g. wind) and sensor noise to preserve reliable performance; the airship should stay as level as possible to avoid added uncertainties in sensor reading; and finally, the controller should not be so complex that the required processing power is too large to be implemented on the Raspberry Pi.

Extensive simulation of different possible manoeuvres showed that MPC gave the best tracking performance, however it runs with high computational complexity which may exceed the capacity of the Pi. Without a complete set of all navigation code intended to run on board the airship, it is not possible to determine if the required processing power is excessive. If this is the case, the H_∞ controller can be used in the system instead - it still provides good tracking but is much less expensive to run on the hardware. LQR also gave a very good tracking response without excessive actuation and since it uses gains that only need to be computed once, it is not computationally expensive. However, LQR optimises performance over robustness, which might invalidate it in the real system.

H SUCCESSFUL AUTONOMOUS FLIGHTS ON VARIOUS UNSEEN MAPS

We tested the autonomous navigation of the airship on several different maps to verify its viability. This ranged from a simple, to complex, to a map representing an Open Day at Imperial College London. Samples of this and the flight path taken is shown in Figures 13, 14 and 15 below.

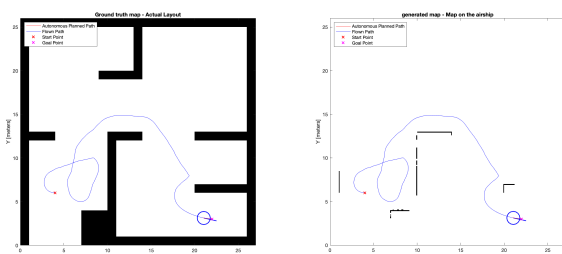


Fig. 13: Autonomous flight in simple map

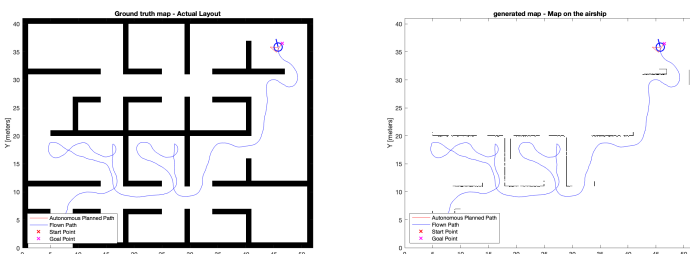


Fig. 14: Autonomous flight in complex map

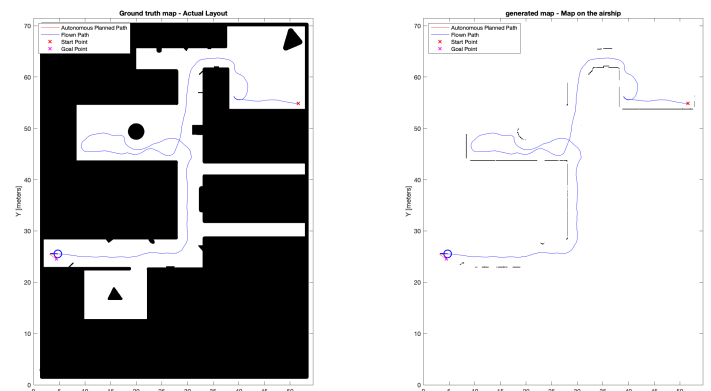


Fig. 15: Autonomous flight in Imperial College map